STUDIES OF HIGH LIFT/DRAG RATIO HYPERSONIC CONFIGURATIONS

JOHN V. BECKER
Langley Research Center
Langley Station, Hampton, Virginia

ABSTRACT

The comparative performance and heat-transfer problems of a variety of simple lifting forms are investigated in the Mach range from 5 to 20. In general it is found that the use of flat lifting surfaces produces higher lift/drag ratios than circular, vee, "caret," and "isentropic compression" surfaces. An exception is the thin delta wing with underslung body for which a favorable interference effect is produced at the lower hypersonic speeds. Configuration limits within which the favorable interference is obtainable are established. As the Mach number advances beyond about 10, adverse viscous interactions develop to such an extent that the interference effect becomes unfavorable, and higher lift/drag ratios are achieved by flat-bottom wing-bodies. A comparison of the best of these wing-body combinations with thick wings and with merged wing-bodies of equal volume and planform area reveals only small differences in peak lift/drag ratio. All configurations suffer a major deterioration in lift/drag as the Mach number is increased and the Reynolds number is decreased in conformance to typical hypersonic flight trajectories, because of the growth of adverse viscous effects. An important factor in this performance degradation is the unexpectedly high pressure found on the lee side at the higher Mach numbers. Heat-transfer studies reveal several anomalies associated with the viscous interactions and with the interacting flow fields of wing and body. An analysis of the leading-edge region of a typical wing leads to the conclusion that the relatively sharp leading edges essential to high lift/drag ratio are not impractical if a combination of internal and radiative cooling techniques are employed.

INTRODUCTION

During the next decade there will be an upsurge of interest in the development of hypersonic vehicles capable of efficient long-range flight within the earth's atmosphere. The speeds of interest range upward from

about Mach 6 for hypersonic transports and recoverable first-stage boosters to near-orbital speeds for boost-glide and advanced self-propelled types. In contrast to the extensive effort that has been and continues to be applied to the aerodynamics of turbojet vehicles in the speed range up to about Mach 3, research on efficient hypersonic forms is still in its infancy.

As a first approach to the hypersonic problem it is pertinent to examine the principles and guidelines which have been established for the lower supersonic speeds. The oldest principle, which up to now has been used almost universally, is separation of the vehicle into discrete elements according to function—the wing for lifting, the fuselage for housing, and so on. As design speeds advanced, increasing refinement in the shape details of these elements and their relative configurational positions became necessary. The swept-wing principle was developed, followed by the transonic and supersonic area rules [1–3]. A direct application of these principles to hypersonic velocities is rather obviously invalid, and results in configurations in which the wing is so highly swept that it tends to be largely engulfed by the fuselage. Thus the old guidelines become virtually useless. At best, they may be interpreted as pointing toward a merging of the wing and body functions. This is evidenced in the lifting-bodies and blended wing-body forms which are of interest in current hypersonic research.

These wingless slender body shapes are all very well for expendable missiles; however, the manned hypersonic vehicles of the future as currently visualized will be required to perform acceptably through the entire flight-speed regime including the conventional low-speed approach and landing. Clearly, then, either the slender body configurations must be equipped with variable geometry devices such as retractable wings, or we must develop fixed geometry configurations having sufficient span to be flyable at low speeds. Accordingly, winged configurations continue to be of great interest in hypersonic research, despite the fact that they cannot be fitted into the geometrical patterns required by the old guiding principles. Toward the eventual establishment of new principles for the design of efficient hypersonic configurations we have studied the comparative performance and heat-transfer problems of a variety of simple wing, body, wing-body, and merged or blended forms in the speed range up to Mach 20. The aim of this paper is to review the principal results obtained so far from these studies.

TWO-DIMENSIONAL PLATES

The flat plate of zero thickness and infinite span is of special interest because its lift/drag characteristics represent an upper limit to the efficiency attainable for hypersonic lifting forms and because it can be analyzed

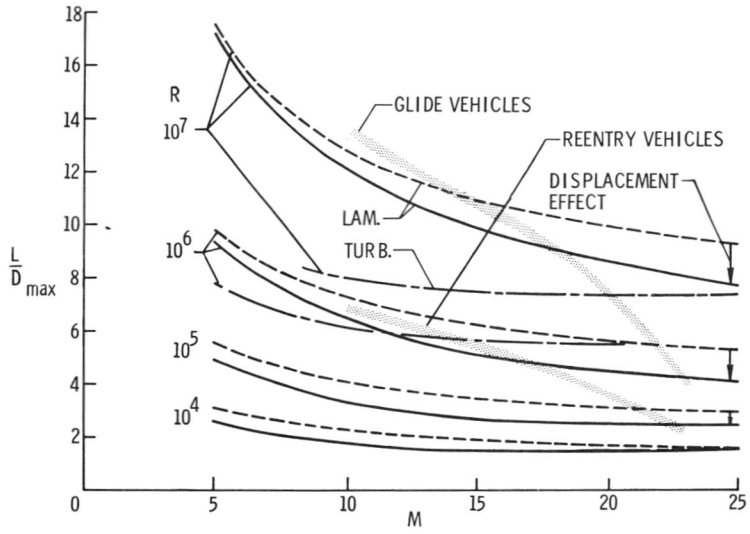

Figure 1. Theoretical lift/drag ratios of two-dimensional flat plates. $T_w = 2500°R$.

theoretically. A great deal of study has been devoted to the complex viscous interaction effects which exert major influences on the lift and drag properties of the plate. If Bertram's analysis [4,5] is used it is found rather surprisingly that the large incremental lift and drag effects due to boundary-layer displacement essentially cancel in evaluating the lift/drag ratio. A basic assumption in the calculation is that the boundary layer on the lifting plate can be treated as one on a plate at zero incidence in a free stream whose properties are the same as those on the inclined plate in inviscid flow. An alternate approach has recently been proposed by White [6] in which the local incidence of the displaced flow is taken as the sum of the plate angle of attack in the actual free stream and the boundary-layer displacement surface slope. With this assumption, a significant deterioration of the L/D due to displacement effects is obtained.* Bertram has recently studied this discrepancy and has concluded that White's approach is the more nearly correct one.

Results obtained with White's assumption are shown as solid lines on Fig. 1. Inclusion of the displacement effects is seen to reduce the L/D_{max} by as much as 20 percent at the higher Mach numbers. The decreasing Reynolds numbers characteristic of hypersonic vehicles as the Mach number advances causes a large degeneration in the attainable L/D. In the

* Symbols are defined in the Appendix.

region of Mach 20 to 22 which is critical for reentry and long-range glide vehicles, these "ideal" L/D values extend from about 3 for the Reynolds numbers of typical reentry vehicles to about 7 for Reynolds numbers an order of magnitude greater. If the various additional losses of real vehicles are considered, the attainable L/D values are typically about half of these flat plate values.

Another region of great interest is found from Mach 5 to 8 which now appears to be the most probable zone of operating speeds for future air-breathing hypersonic-cruising vehicles. Here the ideal maximum L/D values are two to three times higher than the Mach 20 values, principally because of the large favorable effect of much higher vehicle Reynolds numbers, and partly because of the effect of the lower Mach number.

Another point to be noted in Fig. 1 is the comparative performance of the laminar and turbulent cases. Because the turbulent skin friction coefficient diminishes much more rapidly with Mach number than the laminar coefficient [7] the calculated turbulent and laminar L/D values become equal at the higher hypersonic Mach numbers, e.g., at $M = 21$, $R = 10^6$. For lower Reynolds numbers where the turbulent theory predicts L/D values greater than the laminar ones it is generally assumed that only the laminar values have any physical reality. These results are important both in vehicle design and in the interpretation of experimental hypersonic data. Thus in many instances at these high hypersonic Mach numbers the performance is not strongly affected, irrespective of which type of boundary layer prevails. At Mach 5 to 8, however, the same pressures that have traditionally existed in aeronautics to encourage laminar flow still persist. In fact, a major additional incentive is present, namely, the proportionately lower heating rates of laminar flow. In hypersonic testing in the lower speed regime a knowledge of whether the flows are laminar, transitional, or turbulent is vital, and any experiments in which this consideration is neglected must be regarded with suspicion.

Although Newtonian theory clearly reveals the sharp-edged flat lifting surface to be optimum [8] it has often been speculated that an improved surface might be found when the real shock-expansion flows are examined in detail, Ref. 9, for example. The "isentropic" compression surfaces which have been employed successfully in the air-induction problem [10] are of particular interest in this problem. As compared to the flat lifting surface, this shape benefits from the higher local pressures that exist as a result of reduced shock losses. We have recently analyzed the performance of appropriately curved lifting surfaces at Mach 20. For inviscid conditions on both plates and wedges it was found that the curved configurations produced some small gains in L/D_{max}, but only in the area of high $C_{L_{opt}}$, i.e., low L/D_{max}. When viscous effects were included, the results shown on

Fig. 2 were obtained for wedge sections. Except at very low Reynolds numbers and low L/D's, the curved configurations were inferior. The small gains shown theoretically here are considered questionable because of the probable occurrence of flow-separation effects in real flows due to the large adverse pressure gradients on the curved plates. And thus our search for an improvement on the flat hypersonic lifting surface has so far proved disappointing. We believe, however, that some further study in this area is warranted.

WINGS AND BODIES

We now consider the extent to which the ideal lift/drag ratios of the two-dimensional plate are degraded when we proceed to finite shapes. For present purposes we will consider primarily two wing families which theoretically have good prospects for high lift/drag ratio properties at hypersonic speeds, namely, the simple sharp-edged wedges of rectangular and triangular planform. The thickness ratios of interest for these wings range from the lower limit of what is physically feasible ($t/c \approx 0.02$) to the much higher values characteristic of all-wing or blended wing-body configurations ($t/c \approx 0.2$). In hypersonic configuration development we usually seek to house a payload of specified volume within the lifting object of least surface area for the required L/D, because crudely speaking, both the weight of the external heat-protecting structure and the skin friction are proportional

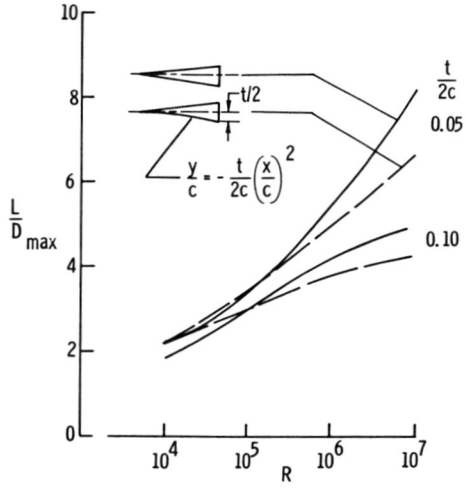

Figure 2. Effect of isentropic compression on the performance of wedges. $M = 20$, $T_w/T_\infty = 6$.

to the area. The nondimensional volume parameter $V^{2/3}/S$ therefore has some meaning as the independent variable in L/D comparisons. For the simple wing forms of interest here, if S is defined as the planform area, this parameter is related to the thickness ratio and aspect ratio as follows:

$$\frac{V^{2/3}}{S} = k \frac{(t/c)^{2/3}}{(AR)^{1/3}}$$

where $k = 0.63$ for the simple wedge of rectangular cross section, and $k = 0.76$ for wedges of triangular or diamond cross section.

These families of simple sharp-edged wedge wings have been investigated at $M = 6.8$ and results recently obtained by Penland together with earlier data [11,12] are compared on Fig. 3 for $R = 1.5 \times 10^6$. This root-chord Reynolds number was chosen as being sufficiently low that the effects of transition, which are believed to exist in some cases at the rear of the wings, would not significantly affect the performance data. The results show a large drop in performance from the comparable two-dimensional plate wing* for even the thinnest practical flat-bottomed wings of relatively high aspect ratio. The experimental data for the flat-bottom delta "roof" family (Fig. 3*a*) are in reasonable agreement with the trends shown by the shock-expansion theory (including displacement effects on the frictional drag component), both as regards the effects of thickness ratio and sweep variations. However, the theory characteristically overestimates the level of the experimental data for these delta wings. In all cases the roof-shaped wings suffered a loss in L/D_{max} when they were tested in the inverted position (not shown), a result in consonance with Newtonian theory.

The rectangular wings (Fig. 3*b*) exhibit better agreement between theory and experiment and their L/D values are superior to those of the roof-shaped delta wings of equal root chord, in spite of the fact that their thickness is somewhat greater for equal volume parameter and equal aspect ratio. (Compare the rectangular wings of aspect ratio 1 and 0.35 (Fig. 3*b*) with the equivalent delta wings of sweep 75° and 85° (Fig. 3*a*).) The principal reason for this is the lower average Reynolds number of the delta wings for equal root chords.† Some further reduction in aspect ratio (improvement in $V^{2/3}/S$) is possible beyond $AR = 0.35$ without serious loss in L/D_{max} for the rectangular wings; however, they then tend to lose their identity as wings and assume the proportions that characterize bodies.

* The L/D of the flat plate for this comparison was computed as in Fig. 1 except that wall and stream temperatures appropriate to the wind tunnel rather than to flight conditions were used.

† From the vehicle designer's viewpoint it is probably more significant to compare delta and rectangular wings of equal planform area and volume. This is done later (Fig. 13).

An inverted vee or "caret" type wing [9] was also tested for comparison with its corresponding rectangular wedge wing (Fig. 3*b*). The inviscid shock location for a two-dimensional surface at an angle of attack equal to α_{opt} for the wing of $AR = 1$ was used to design the pressure side of the caret wing. The aspect ratio and thickness ratio of the rectangular wing were

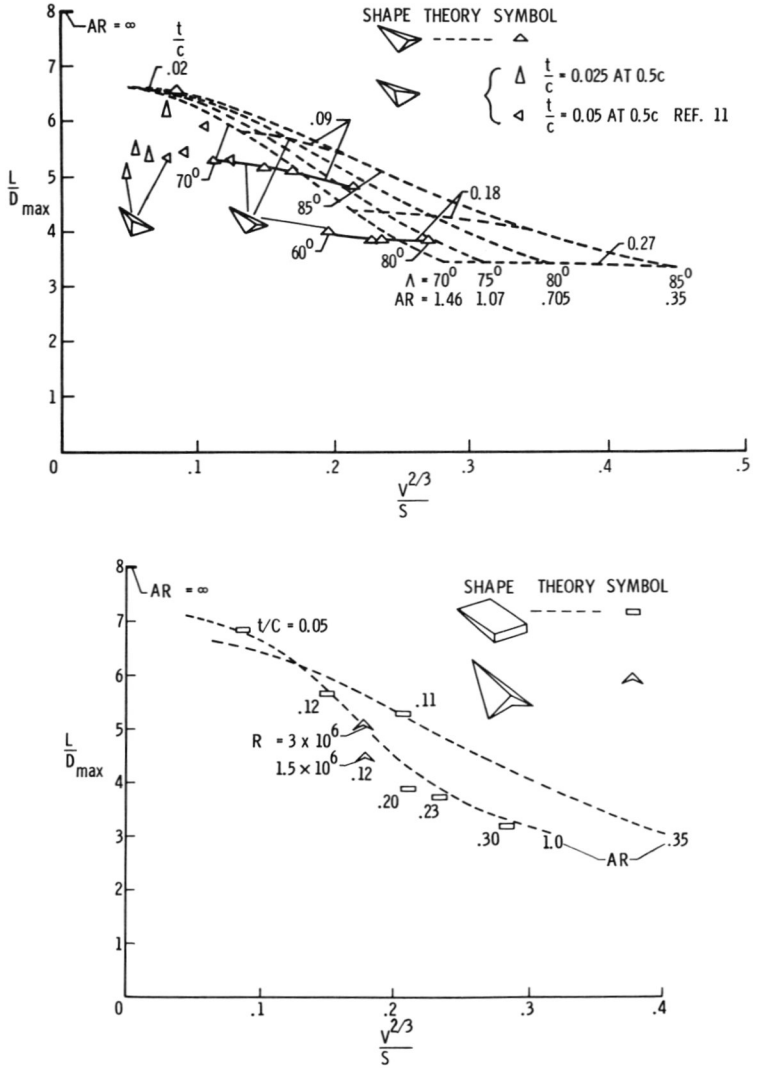

Figure 3. Performance of sharp-edged wing families. $M = 6.8$. (*a*) Delta wings. $R = 1.5 \times 10^6$. (*b*) Rectangular and caret wings. $R = 1.5 \times 10^6$ except as noted.

duplicated in the caret wing. The lower point on Fig. 3*b* is for a caret wing of the same root chord as the rectangular wing. The upper caret point labeled $R = 3 \times 10^6$ is of greater interest for comparison because it represents a wing of the same projected planform area as the rectangular wing. While the L/D_{max} of the caret wing in this latter comparison is less than the rectangular wing of equal t/c, AR, and area, its volume is somewhat greater. For equal volume and equal area the upper caret point is seen to fall on the same curve as the rectangular wings. A direct comparison of caret and flat-bottomed deltas of equal t/c and planform was not made, but interpolation of the flat-bottomed wing data of fig. 3*a* reveals approximately equal performance. Thus for equal volume and area there is clearly no deterioration in performance when the inverted vee bottom shape is used in the form specified by the simple caret concept. On the other hand, there is no apparent improvement either, such as has been hinted at in some of the literature.

It is currently popular to call any hypersonic configuration which does not exhibit a well-defined thin wing a "lifting body." We find it useful, however, to employ a more restrictive definition which considers only axisymmetric bodies, their corresponding half bodies, and similar nonaxisymmetric shapes whose maximum width does not exceed twice the maximum depth. As in the case of the wings, our results for bodies at $M = 6.8$ indicate that a length Reynolds number of about 1.5×10^6 is about the highest value to which predominantly laminar L/D properties can be maintained. Figure 4*a* compares several body series at these conditions [13–17]; and Fig. 4*b* shows preliminary data uncorrected for base pressure obtained recently by Johnston and Woods in the Langley Helium Tunnel at $M = 20$ and $R = 3.5 \times 10^6$. For reasons given previously it is believed that the Mach 20 results at this higher Reynolds number also exhibit essentially laminar behavior.*

In general, the width and depth dimensions of a body vary simultaneously when the fineness ratio is changed, and the volume parameter thus decreases as the body becomes more slender. This is in contrast to the wings of fixed thickness ratio for which the volume parameter, as we have seen, increases as the planform shapes become more slender. For the cone as an example,

$$\frac{V^{2/3}}{S} = 1.03 \tan^{1/3} \theta$$

* The use of helium raises some other questions if it is desired to correct the helium data in order to indicate the equivalent performance in air [18–20]. For our present purposes we are concerned chiefly with the comparative results shown on Fig. 4*b* rather than the absolute values. It may be added, however, that satisfying agreement with air-tunnel L/D data for simple configurations has been achieved when straightforward corrections are applied for the differences in lift-curve slope and skin friction between air and helium.

where θ is the half angle. As θ and $V^{2/3}/S$ are reduced a point of peak L/D is obtained beyond which the L/D starts to diminish because of the decay in lifting effectiveness at very low planform aspect ratios. This is clearly seen for the half cones in the vicinity of $V^{2/3}/S \approx 0.3$ in Fig. 4. The dashed-line extrapolation of the full-cone data is based on a Newtonian calculation which also indicates the possible occurrence of a peak for full cones in the same region of slenderness. If the thickness of the body is reduced and its

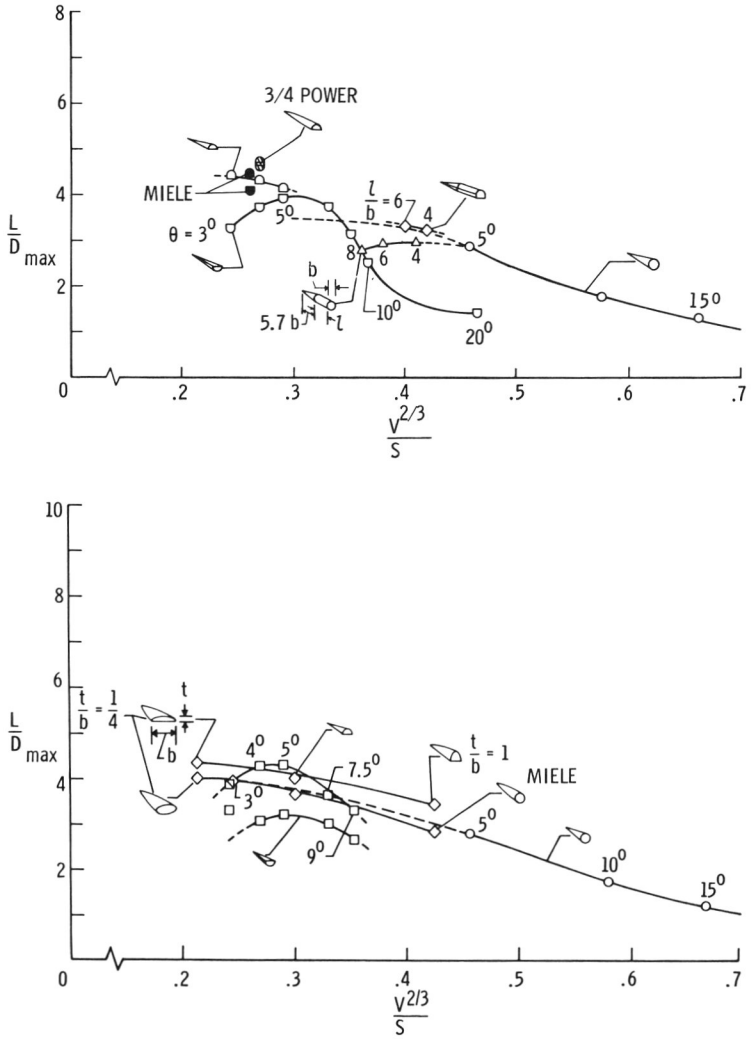

Figure 4. Performance of pointed bodies. (*a*) $M = 6.8$, $R = 1.5 \times 10^6$. (*b*) $M = 20$, $R = 3.5 \times 10^6$, helium.

width increased so as to maintain constant streamwise cross-sectional area distribution, as in the case of the bodies of minimum-drag area distribution on Fig. 4*b*, the shapes then become progressively more winglike and the L/D increases continuously as the volume parameter diminishes in a manner similar to the wings of decreasing thickness.

Although it is not clear that the theoretically optimum area distributions determined for nonlifting axisymmetric bodies apply also to lifting conditions, our results (Fig. 4) do indicate that such shapes have generally better performance than cones or half-cones of equal $V^{2/3}/S$. The $\frac{3}{4}$-power body [21] is optimized for specified length and diameter. The Miele shapes [15, 16] are optimized for specified volume and length; they are thus more blunt in the forebody region and have somewhat higher drag than the $\frac{3}{4}$-power shape, but at the same time they are more attractive from the point of view of practical volume distribution and usability of the available volume.

It is clear that axisymmetric bodies—optimized or not—have inferior L/D characteristics. All of the flat-bottomed bodies in Fig. 4 were found to have higher L/D values when compared to the corresponding round-bottom shapes. Figure 5 summarizes our work and other pertinent data on this point [14,20,22,23]. In all cases on Fig. 5 the comparisons involve the same body tested flat side down and nonflat side down so that the area distributions and volume parameters are held constant. It is thus well established that the Newtonian indications for flat-lifting-surface bodies are correct. This is a simple and important guideline for configuration development.

WING-BODY COMBINATIONS

Almost a decade ago when supersonic interference flows were first studied in detail [24], Eggers and Syvertson [25] proposed a simple arrow-wing underslung half-body configuration which provides a practical means of achieving favorable lift interference, the lift of the wing being augmented by the pressure field of the half-body mounted beneath it. They suggested that the wing be sized so as to encompass exactly the body flow field at zero wing incidence. A simple linearized theoretical estimate which considered only lift-interference effects was made and this appeared to be in rough agreement with the first experimental L/D_{max} results at a Mach number of about 5 [25]. Configurations of this general type, usually designated "flat-top," naturally become the subject of more detailed hypersonic research. As a basis of evaluation of the favorable interference effect it is common practice to use the performance obtained with the configuration inverted, which provides a flat-bottom arrangement representing the Newtonian optimum which neglects possible interference effects. The

results of many such experimental comparisons are summarized in Fig. 6 [20,22,25–28]. Many of the configurations included in Fig. 6 did not conform to the "optimum" arrangement suggested in Ref. 25 because the wings had more span than necessary to cover the body flow field, and many of the wings had delta rather than arrow planforms. However, based on the simple lift-interference concept of Ref. 25, all would be potentially capable of some degree of favorable interference. In general, the desired effect has been found only at the lower hypersonic speeds, and it seems to disappear at a Mach number of about 10, beyond which the flat-bottom configuration (fuselage on the low-pressure side) is superior. The linearized estimate not

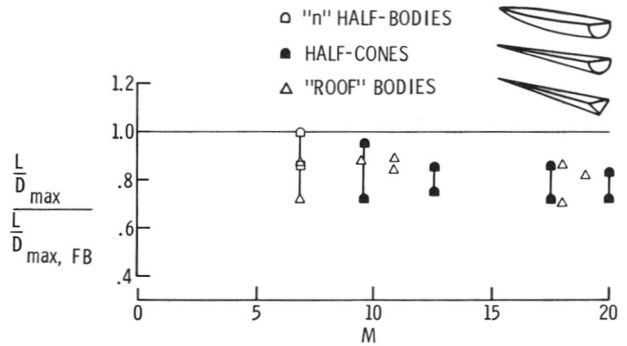

Figure 5. Comparison of the lift/drag ratios of various half bodies in the erect and inverted (flat-bottom) positions.

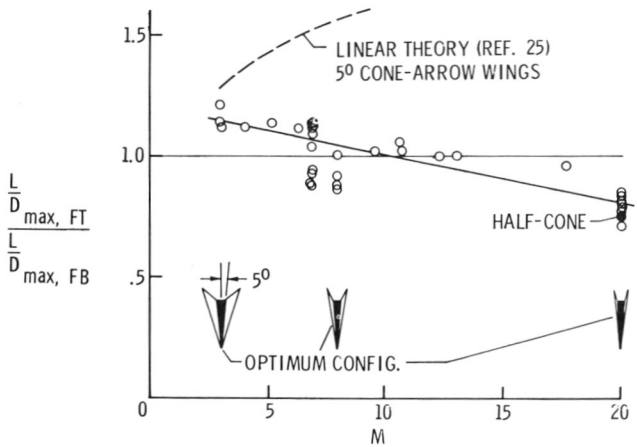

Figure 6. Comparison of the performance of delta-wing half-cone, and arrow-wing half-cone configurations in erect (flat-top) and inverted (flat-bottom) positions.

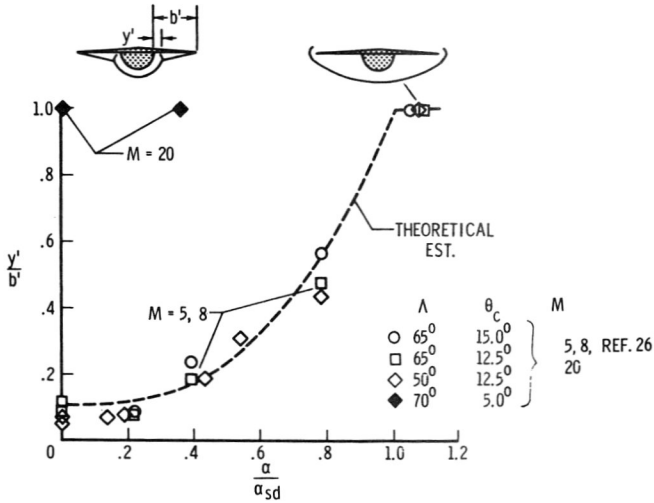

Figure 7. Effect of angle of attack on position of body shock for flat-top configurations. $R \approx 3 \times 10^6$.

unexpectedly is quite inadequate, showing a Mach number trend of the wrong sign. An important and, until recently, mysterious result shown on Fig. 6 is the coexistence at a given Mach number (Mach 7 for example) of flat-top configurations exhibiting large favorable interference and generically similar configurations having large unfavorable interference. We have studied the mechanisms which produce this anomaly with the objectives of explaining the experimental results and of extending the favorable interference effect to higher speeds.

We will examine first the results of pressure distributions at Mach 5, 8 and 20 (from Ref. 26 and the present investigation) to locate the shock position and the nature of its effect on the pressure distributions on wings whose leading edges lie well ahead of the expected body-shock positions. At Mach 5 and 8 clearly defined pressure jumps indicated the shock positions shown on Fig. 7. As the angle of attack increased the shock moved outward, reaching the leading edge at approximately the angle of attack for shock detachment [29]. The outward motion of the shock agrees well with estimates in which the half-cone is assumed to be operating at the diminishing Mach numbers on the wing surface (dashed curve on Fig. 7).* Unfortunately, this orderly picture is spoiled when we add the results of

* With the parameters used in fig. 7, slightly different theoretical curves are obtained for each test configuration; however, these differences are less than the uncertainties in interpretation of the Mach 5 and 8 pressure data and therefore only the estimate for $\Lambda = 50°$, $\theta = 12.5°$, $M = 8$ is shown.

careful pressure measurements at Mach 20 recently obtained by Henderson at Langley. Details of his pressure surveys are given in Fig. 8. There is no evidence of any shock-induced pressure jump on the wing, either on the high pressure side at $\alpha = 0$ or $\alpha = 4.5°$ or on the lee side at $\alpha = 7°$, conditions for which the body shock was expected to be in evidence on the basis of the lower Mach number findings. The pressures are seen to be greatly increased by the presence of the body over the entire side of the wing on which the body was mounted. The character of the pressure distribution is identical to the distributions obtained at the lower Mach numbers [26] for the cases for $\alpha > \alpha_{sd}$ where the body shock has coalesced with the detached bow shock, and thus we have indicated "apparent" shock positions at $y/b = 1$ on Fig. 7. It may be noted that Henderson's configuration for Mach 20 was, to a good approximation, hypersonically "similar" to the 50° swept wing and 12.5° half-cone used at Mach 8 (i.e., the span and thickness dimensions were all smaller in the Mach 20 test by roughly the factor 8/20). The results thus clearly indicate that viscous interaction effects preclude any direct use of the similarity concept as a tool for extrapolation, at least when it is employed over such a wide range of Mach number.

At the large value of the shock interaction parameter of the Mach 20 tests ($\bar{\chi} = 2.2$) the interaction effects evidently dominate the interference flow picture. Whether the thick body and wing boundary layers coalesce in a manner which does not require the presence of a discrete body shock on the wing or whether the boundary layers are so thick as to mask detection of the shock by surface pressure measurements is not yet known. In any case, this large disturbance of the entire pressure field by the body is believed to be a significant factor in the adverse interference effects noted in the L/D values for this type of flat-top configuration at Mach 20 (Fig. 6). Configurations for which the body shock falls at the leading edge may possibly not suffer to the same degree from this problem because no direct interactions occur on the wing surface; however, the effects of interfering thick boundary layers on body and wing are still present of course.

Of particular interest for the flat-bottom configuration are the pressure surveys of Fig. 8*c* showing the results obtained with the body on the low-pressure side of the wing. A pressure level of about 6.5 times the stream pressure is observed, a large fraction of the pressure found on the high-pressure side. Obviously the near-vacuum conditions predicted by inviscid theory are grossly unrealistic, and the actual pressures are several times larger than those of the wing alone. The low-pressure side thus emerges as a key consideration in the L/D problem. Little is known of the nature of these flows and no attempts have yet been made to determine the most effective body shape for this side of the wing.

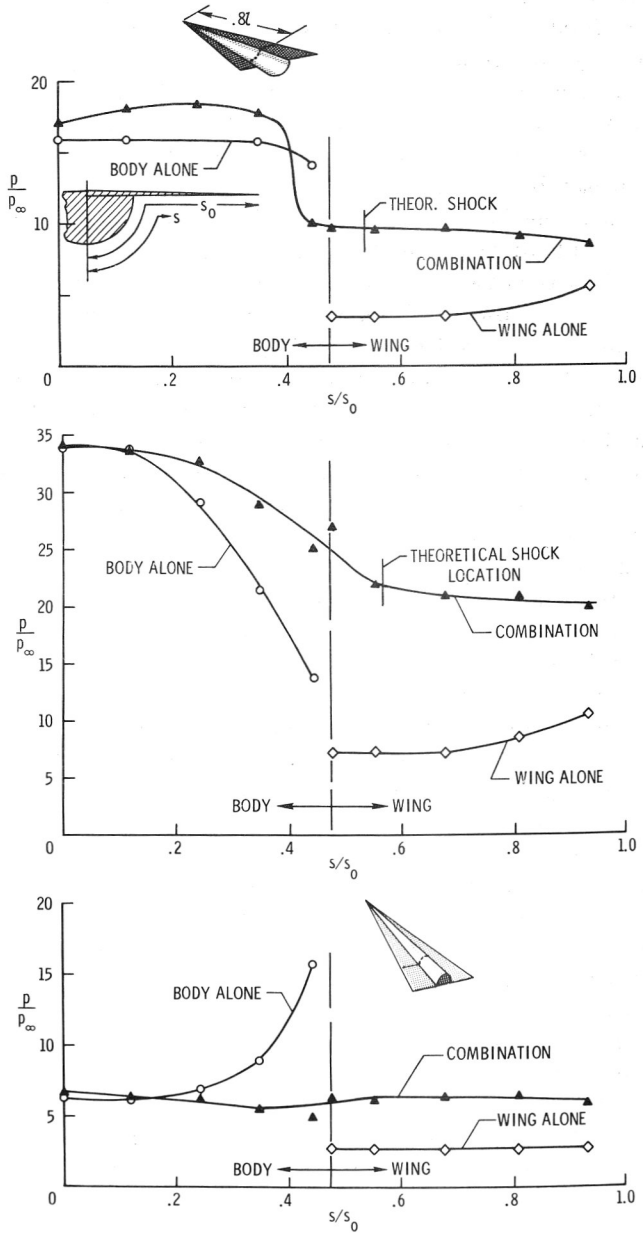

Figure 8. Pressure distributions at Mach 20 in helium. $R = 4.5 \times 10^6$, $\bar{x} = 2.2$, $\Lambda = 70°$, $\theta = 7.5°$. (*a*) Flat top, $\alpha = 0°$. (*b*) Flat top, $\alpha = 4.5°$. (*c*) Flat bottom, $\alpha = 7°$.

Approximate theoretical approaches [28] for flat-top configurations have been proposed for the shock-on-wing case. These methods, of course, neglect boundary-layer interactions of the type noted above. No reliable methods of calculation exist if $\alpha_{opt} > \alpha_{sd}$, i.e., if the shock is detached. The flat-top case for $\alpha \approx \alpha_{sd}$ has been treated approximately [30]. The flat-bottom configuration is difficult to analyze particularly because of large uncertainties about the complex flow on the low-pressure (body) side of the wing. Engineering calculations have been made by various Langley investigators for both types of configuration for the case where the flow is attached at the leading edge. These studies, although differing in detail, all indicate higher lift/drag ratios for the flat-bottom arrangement. However, it is found that as α_{sd}/α_{opt} approaches unity, the calculated L/D advantage of the flat-bottom type diminishes, and the results thus suggest possible superiority of the flat-top design for conditions in the vicinity of or beyond shock detachment. Since this criterion also governs the presence or absence of the large disturbances of the wing flow due to the body shock, Fetterman has analyzed the available experimental L/D data to determine to what extent the results actually do depend upon this parameter. A gross comparison of some of the pertinent L/D data from Fig. 6 for a wide range of conditions (Fig. 9) indicates the anticipated dependence on $\alpha_{sd}/\alpha_{opt,}$* and the flat-top configuration in general tends to be superior only for values of this parameter near or less than unity. The considerable dispersion of the data in Fig. 9 is caused by differences in M, R, and $V^{2/3}/S$. If the effects of M and R are eliminated by examining only data at $M = 6.9$, $R = 1.4 \times 10^6$, the results shown in Fig. 10 are obtained. The flat-top configurations are seen to be superior primarily for the smaller volume ratios and for values of α_{sd}/α_{opt} near or less than unity.

The physical reasons for this behavior include the presence of adverse body-shock interaction effects for the flat-top configurations when $\alpha_{sd} > \alpha_{opt}$ which have already been discussed. Similar effects for the flat-bottom case occur on the low-pressure side of the wing where, presumably, they would be less deleterious. Thus in the region of attached leading-edge flows the flat-bottom cases show superior performance. When the leading-edge shock detaches, additional considerations are involved. In the detached-flow high-pressure air from the under surface of the wing bleeds to the upper surface causing a loss in lift, and in the flat-bottom case an increase in body drag. The lift loss is serious for the flat-bottom configuration because of its relatively high values of α_{opt}, typically 7° to 8°. For the

* The normalizing quantity $\alpha_{opt,FB}$ is used rather than $\alpha_{opt,FT}$ because the analytical work for the flat-bottom cases indicated a strong dependence upon this parameter. Furthermore, $\alpha_{opt,FT}$ usually occurs for the detached-shock condition and cannot be determined accurately by the approximate calculation methods.

flat-top configuration typical values of α_{opt} are much lower, 2° to 3°, and the loss in lift at shock detachment is less serious. Thus the flat-top design tends to be superior if the leading-edge flow is detached.

These results serve partially to explain the Mach number trend in favor of the flat-bottom configuration observed on Fig. 6. To maintain their superiority the flat-top configurations tested should have employed increasing sweep as M increased to maintain $\alpha_{opt} \sim \alpha_{sd}$. The fact that for a majority of the configurations this was not done explains in part the deterioration of the flat-top performance indicated on Fig. 6.

Figure 11 provides, however, a strong indication that the flat-top L/D will never reach or exceed the flat-bottom value at very high Mach numbers ($M \sim 20$) even though "optimum" wing configurations are employed. As the wing sweep diminishes a peak in the ratio of L/D values of only 0.85 is found at a value of α_{sd}/α_{opt} of about 2. And as the sweep is further reduced toward the "optimum condition" of $\alpha_{opt} \sim \alpha_{sd}$ the flat-top performance deteriorates. This failure of the flat-top to exhibit any favorable interference at Mach 20 is presumed to be caused primarily by the large adverse viscous interactions between body and wing flows noted previously. The sketch at the top of Fig. 11 for $\alpha_{opt} = \alpha_{sd}$ suggests that these interactions may produce a large spillage of air from the lower to the upper

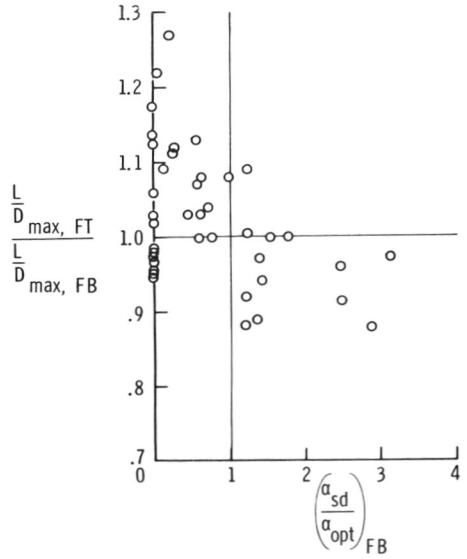

Figure 9. Effect of shock detachment on relative performance of flat-top and flat-bottom cone-delta and cone-arrow wings. $M = 3$ to 10, $R = 0.7$ to 6.1×10^6, $V^{2/3}/S = 0.07$ to 0.28.

surface for the nominally optimum condition. A second contributing cause is the fact that the lift is carried largely by the round-bottomed body when the wings become very small as required for the "optimum" configuration at Mach 20. Thus ultimately at very high Mach numbers the inherently poor lifting efficiency of the round-bottom body will nullify any gains due to favorable wing-body interference. (Note the L/D ratio for conical half-bodies included on Fig. 6 at Mach 20.) It seems probable, however, that

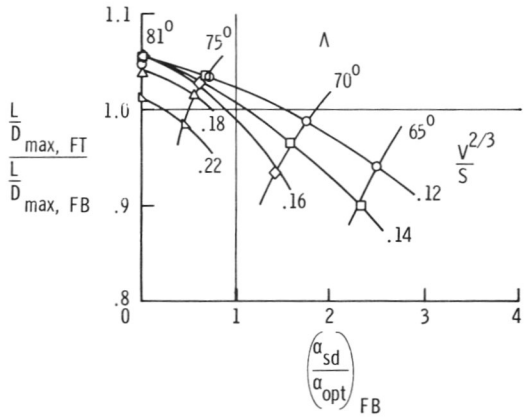

Figure 10. Effect of shock detachment for specific values of sweep and volume parameters. $M = 6.8$, $R = 1.4 \times 10^6$.

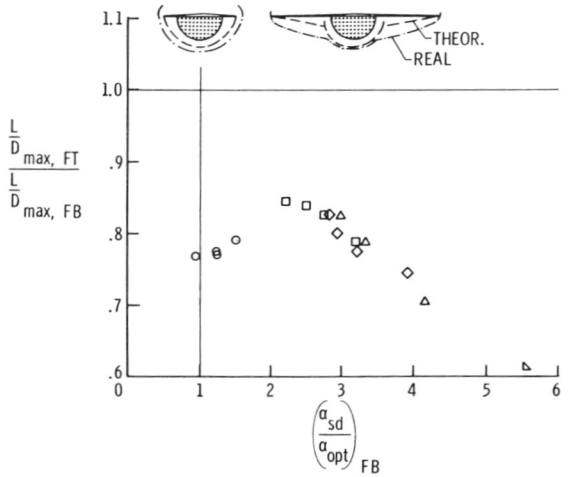

Figure 11. Effect of shock detachment on results obtained in helium at $M = 20$. $R = 3.5 \times 10^6$.

the crossover Mach number of about 10 shown on Fig. 6 can probably be increased if properly optimized wing sweep is utilized.

The hypersonic similarity rules, although admittedly of questionable utility in the presence of large viscous effects, would require that the body thickness as well as the wing thickness and wing span be reduced (in inverse proportion to M) in order to maintain a high L/D level as the Mach number advances. If the similarity requirement were applied literally the optimum 5° half-cone configuration illustrated on Fig. 6 for Mach 8 would have to be slenderized to a 2° half-cone and an 86.5° swept wing at Mach 20—rather impractical proportions for which viscous effects would certainly be dominant. Nevertheless, some explorations in this direction should probably be included in any program aimed at preservation of the favorable interference effect.

Recent results (Fig. 12) for wings of extreme sweep have been obtained in our program at Mach 6.8 which provides additional insight into the behavior of these configurations when the body shock falls well upstream from the wing leading edge. It is seen that the region of favorable interference for the flat-top is limited to a small range of sweeps centering on the geometry for which $\alpha_{opt} \sim \alpha_{sd}$. Deep in the detached shock region where the wing lift becomes small in relation to the body lift the flat-bottom becomes markedly superior.

We have explored here only a limited number of shapes for the body component of these discrete wing-body combinations (mostly half-cones). There are several other interesting forms, including modified pyramidal and parallel-sided shapes for which there are possibilities of enhancing the favorable interference effect in the lower hypersonic range.

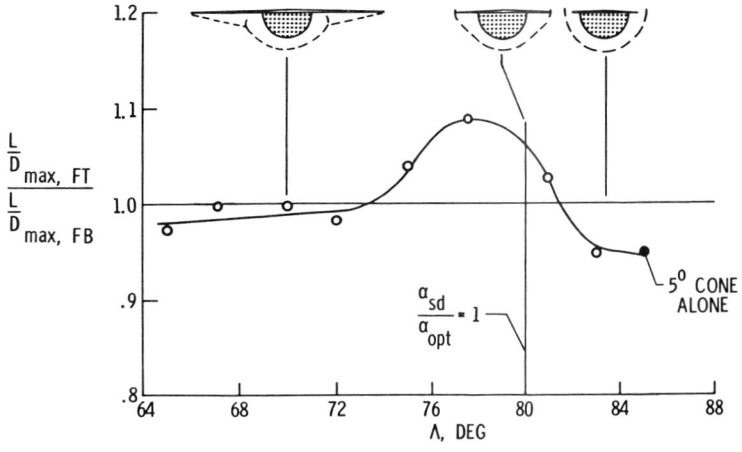

Figure 12. Details of effects of sweep for 5° half-cone configurations. $M = 6.8$, $R = 1.4 \times 10^6$.

MERGED CONFIGURATIONS

So far we have dealt with the discrete wing-body combinations by showing only the comparative behaviors of equivalent flat-top and flat-bottom designs. It is of interest now to examine the actual values of L/D_{max} for a few of these configurations having the proportions indicated by the preceding analysis to be optimum or near optimum, i.e., configurations for which $\alpha_{opt} \sim \alpha_{sd}$. We will compare the performance so achieved with that of the best of the flat-bottom wing and body forms in which the lifting and volume functions have been combined—i.e., in which sufficient thickness is incorporated to produce the same values of the volume parameter as for the discrete wing-bodies. For the latter shapes we will show only the upper envelopes of performance indicated by Figs. 3 and 4 to be actually achievable at $R = 1.5 \times 10^6$. These comparisons are shown in Fig. 13. It is evident at a glance that the flat-bottom wing-bodies have nearly the same performance as thick wings of equal $V^{2/3}/S$. The lower-Reynolds-number line for the rectangular wings is the more significant of the two shown in this comparison because it represents wings of the same area and same volume (rather than the same root chord) as the delta wings and wing-body combinations. Some of the flat-top wing-bodies enjoying favorable interference are capable of small improvements over the flat-bottom delta wing

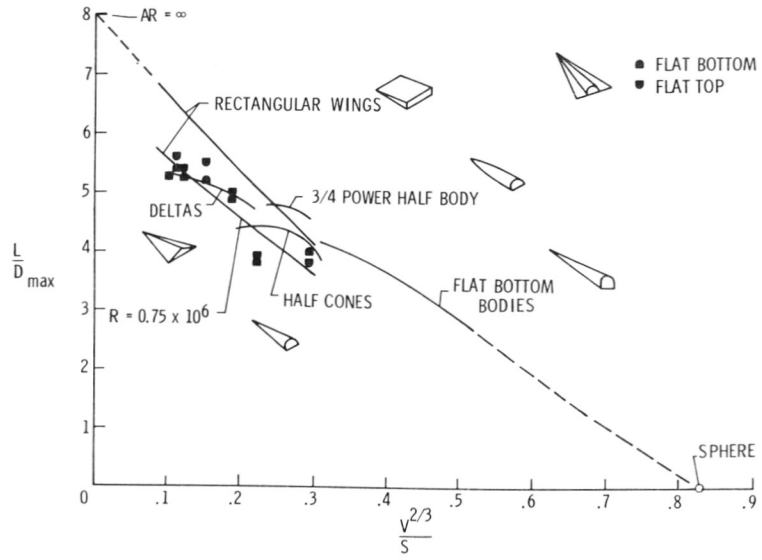

Figure 13. Performance comparison of half-cone delta-wing configurations of near-optimum proportions and the best flat-bottom wings and half bodies of Figs. 3 and 4, at equal $V^{2/3}/S$. $M = 6.8$, $R = 1.5 \times 10^6$ (except as noted).

results at low values of $V^{2/3}/S$. At large values of the volume parameter (0.25 or greater) the discrete-wing bodies have large cone angles and relatively small wings, and for reasons given previously, they do not compare favorably with either the thick delta wings or the slender lifting bodies.

Further comparisons of this kind are presented in Fig. 14 for Reynolds numbers in the transitional range and for a series of shapes in which nearly equal volume parameters were employed in the tests for the delta-roof and delta-half-cone shapes, both erect and inverted. Also shown are comparative results for delta-half-cone and delta-blended shapes at Mach 8 from Ref. 26. These comparisons like those of Fig. 13 indicate no significant advantage for the merged or blended forms.

HEATING STUDIES

After several decades of research it is still not possible to predict in any exact detail the local characteristics of the boundary layer on lifting aerodynamic vehicles. At subsonic and at lower supersonic speeds satisfactory flight vehicles have been developed in spite of this situation, largely because an exact knowledge of the local boundary-layer friction or heating is unnecessary at the lower speeds. In the hypersonic-speed regime, however, precise knowledge of local phenomena is vital to success because we

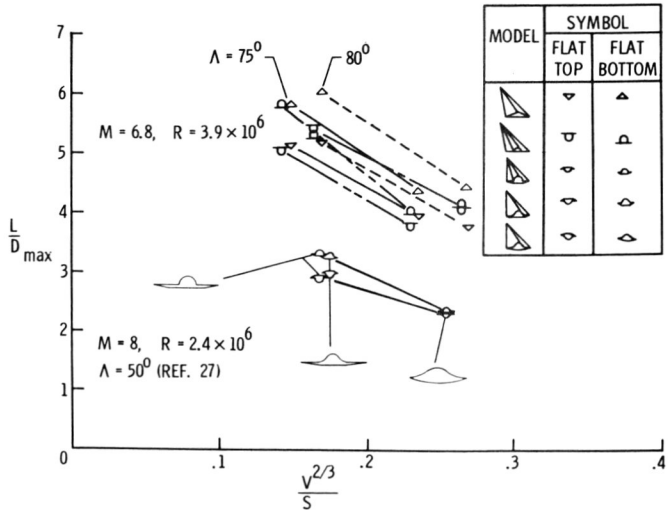

Figure 14. Effects of merging on L/D_{max}.

are concerned now with predictions of local heating, which if not correct in detail, can result in structural failure.

Extensive hypersonic heating studies have been carried out for delta wings (Ref. 27, for example). Strip-theory techniques at the lower angles of attack and cross-flow methods for high angles afford approximations to the correct local heat transfer, provided they are used in conjunction with measured pressure distributions. One of the early superstitions regarding hypersonic flow—namely, that only laminar boundary layers would prevail because of the stabilizing effects of the relatively cool surface—has now been thoroughly discredited, at least for the lower hypersonic range. A Langley study of a 75° delta wing emphasizes this point (Fig. 15). We see clearly that transition starts at a local Reynolds number of about 0.5×10^6 near the edges and 0.7×10^6 on the centerline. Referring to the typical vehicle Reynolds numbers of Fig. 1 we can conclude from these results that transitional flows will constitute a prime problem of heat transfer to hypersonic vehicles. The problem will be complicated by the superimposed uncertainties of surface distortions.

Theoretical work on the heat transfer to bodies [31–36] has provided a framework principally for nonlifting conditions and for conditions of high lift where cross-flow methods become valid. Unfortunately, the attitudes for peak L/D lie midway between these two flow regimes. Thus, for the present at least, we must rely heavily on experiment to obtain the necessary knowledge of heat transfer to lifting bodies in the vicinity of peak L/D.

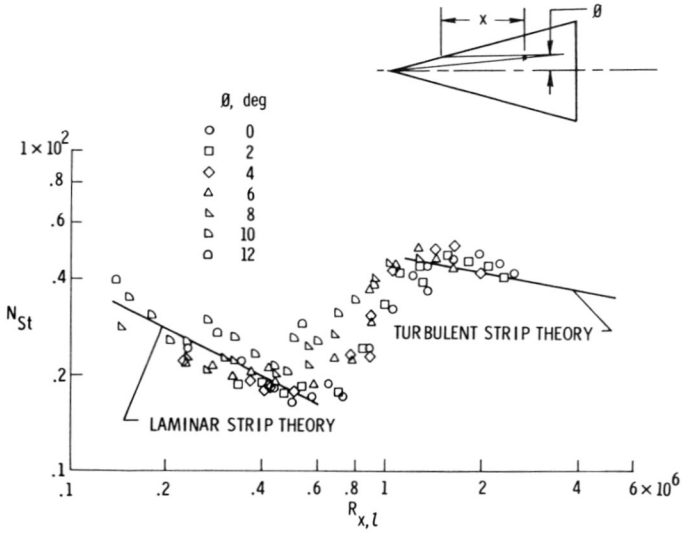

Figure 15. Heat-transfer data for pressure side of sharp-edged delta wing showing transition at low local Reynolds numbers. $\Lambda = 75°$, $\alpha = 16°$, $M = 6.8$, $T_w/T_\infty \approx 5$.

The discrete wing-body combination is a still more complex problem. We have recently studied the heat transfer to the half-cone delta-wing configuration at Mach 6.8 and 9.6. Results obtained by Dunavant for the lower centerline of the body are shown in Fig. 16. The flow at the dividing streamline of the cone remains laminar throughout the α range at the relatively high free-stream Reynolds number of 3.1 million. The character of the flow changes gradually from conical to cross-flow.

Heating rate distributions over the body and wing at $\alpha = 0$, $M = 9.6$ are shown in Fig. 17. An interesting large departure from expectations was discovered on the side of the cone where the heat rate is nearly double the predicted cone value. This phenomenon occurs in the vicinity of the intersection of the wing shocks and the body and is perhaps due to a vortex formation at this discontinuity. An oil-flow photograph (Fig. 18) illustrates clearly the presence of such a phenomenon. Thus we find rather clear evidence of the presence of the wing shock from these heat-transfer and flow data, whereas effects attributable to such a shock were not detected in the pressure data (Fig. 8). A region of low shear and low heating, possibly indicating flow separation, exists in the wing-body juncture (evident on Fig. 18 by the undisturbed ink dots). Previous Langley studies of heating in the juncture of two mutually perpendicular flat plates revealed a similar region of low heating [27, 37]. These results apply for Reynolds numbers low enough to avoid significant complications due to transition.

As the Reynolds number is increased the heating picture changes drastically as shown in the next illustration, Fig. 19, for an angle of attack of 11°. The shock interaction and juncture flow phenomena promote a some-

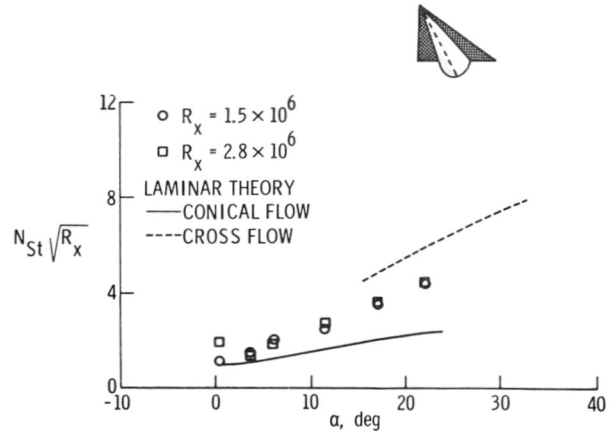

Figure 16. Comparison of heat-transfer correlating parameter measured on cone with laminar theory using measured pressures. $M = 6.8$, $R = 3.1 \times 10^6$, $T_w/T_\infty \approx 5$.

what earlier transition than for the isolated wing (Fig. 15). The turbulence spreads gradually over the entire wing. Only the central area of the body remains laminar. It is clear that hypersonic vehicle designers will have to deal with heat-transfer problems aggravated by the complexities of transitional flows. The prediction of hypersonic heating rates for fully developed turbulent flow is presently uncertain even for the flat plate case because of the semiempirical nature of the available extrapolation formulas.

Closer examination of Fig. 19 and other results at angles of attack near α_{opt} reveal the juncture flow phenomena to be extremely complex, under some circumstances producing hot spots on the wing as contrasted to the

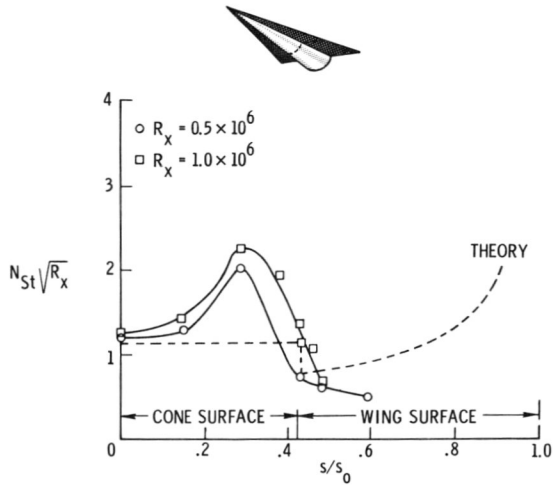

Figure 17. Comparison of distribution of heat-transfer correlating parameter at $\alpha \approx 0°$ with laminar-strip theory. $M = 9.6$, $R = 1.1 \times 10^6$, $T_w/T_\infty \approx 6$.

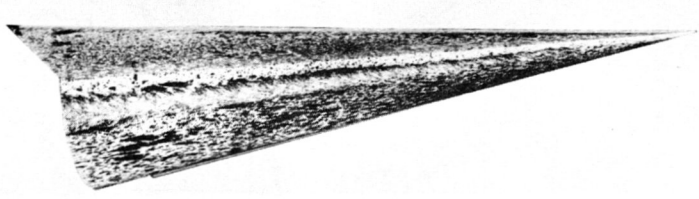

Figure 18. Ink-flow photograph showing type of disturbance on side of cone giving rise to peak heat transfer shown on Fig. 17. $\alpha = 0°$, $M = 20$, helium. (Pressures on Fig. 8*a*.)

reduced heating at zero angle of attack (Fig. 18). An interesting illustration of this at Mach 20 is shown in oil-flow photographs obtained by Henderson for a flat-top configuration at $\alpha \sim \alpha_{opt}$ (Fig. 20). The flow on the body is seen to be deflected downward onto the wing creating a region just outboard of the juncture where mixing with the wing flow produces the region of high shear and high heating. It was thought at first that the outboard boundary of this region was perhaps determined by the body shock. However, failure to find any evidence of the body shock in the Mach-20 pressure data, together with the fact that the width of the high-shear region does not change appreciably with angle of attack, leads us to believe that the phenomenon is essentially independent of body-shock interference effects.

Thus we see that location of the body on the lower side of the wing aggravates the heat protection problem in two ways. Basically this is a region of high heating requiring external heat protection for the body comparable to that of the high-pressure side of the wing. Second, the presence of the body increases the heat load both through its adverse effect on transition and through flow interactions of the type shown in Fig. 20. If the body contains passengers or equipment requiring a low temperature environment the provision of adequate internal insulation will prove to be an additional difficult problem [38]. These difficulties can be alleviated by

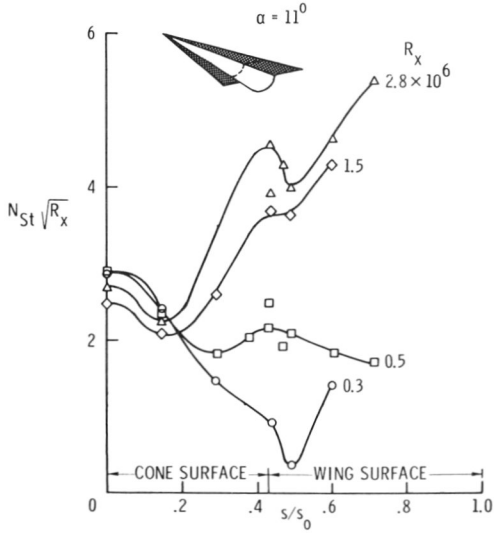

Figure 19. Spanwise distribution of heat transfer on delta-wing half-cone combination at $\alpha \approx 11°$. $M = 6.8$, $T_w/T_\infty \approx 5$.

location of the body on the top or low-pressure side of the wing. Figure 21 indicates the large reductions in heating on the exposed surface of the body that are possible, even at low angles of attack appropriate to high L/D. (The part of the top-mounted body that is buried in the wing may be subject to the high heating rates of the under surface of the wing, but the surface area involved is always less than the exposed cone surface subject to high heating in the underslung configuration.) Furthermore, the upper body location is compatible with the requirements for high L/D at the higher hypersonic speeds as discussed previously.

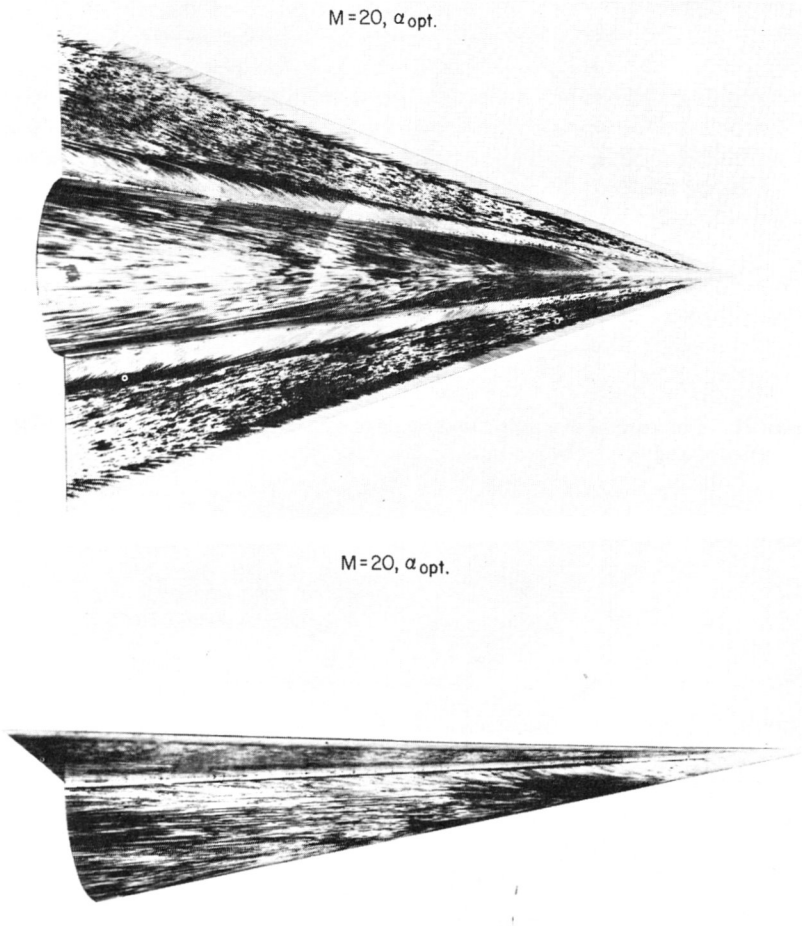

Figure 20. Flow on body side of flat-top configuration for shock-on-wing condition, $\alpha = 4.5°$. $M = 20$, helium. (Corresponding pressures on Fig. 8*b*.) (*a*) Bottom view. (*b*) Side view.

Consideration of heat protection techniques in any detail is beyond the scope of this paper. However, it is in order to consider whether the configurations required for high L/D indicated by these aerodynamic studies are within reach or totally impractical. It is readily apparent from the enormous total heat loads generated in long-range high-L/D gliding flight that there is no hope of absorbing the total heat load in a coolant system or in an ablation material. Radiation of a major fraction of the total heat load from high-temperature external surfaces offers the only presently workable technique for high-L/D vehicles. This technique unfortunately is not adequate for the wing leading-edge regions of the high-L/D con-

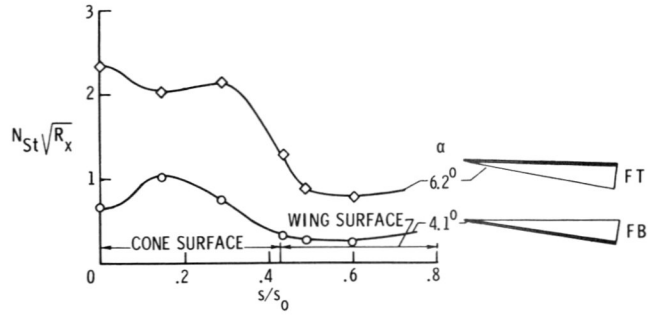

Figure 21. Comparison of heating on body side of flat-top and flat-bottom configurations at angles of attack near α_{opt}, $M = 9.6$, $R_x = 0.5 \times 10^6$, $T_w/T_\infty = 6$.

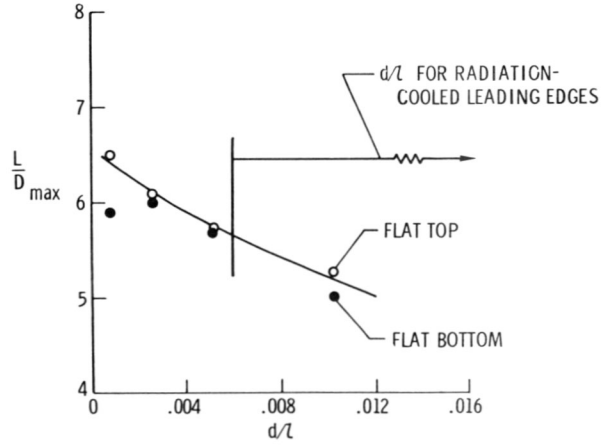

Figure 22. Effect of leading-edge diameter on L/D_{max}, delta-wing power-law half-body, $\Lambda = 78°$, $n = 1/2$. $M = 6.8$, $R = 3.6 \times 10^6$.

figurations discussed previously. Excessive temperatures will develop in this region with radiative cooling alone. The technique of enlarging the leading edge to reduce its heat rate cannot be employed successfully in this problem because leading edges for highly swept wings of the order of 1 ft in diameter are required. The disastrous effect of such dimensions on the L/D is indicated on Fig. 22.

The only possibilities for heat protection of high-L/D forms thus lie either in the development of vastly improved materials, or in the use of general radiative cooling plus local internal cooling in hot-spot areas such as the leading edge. We have analyzed the latter case in some detail to determine the coolant requirements and will now review briefly our more pertinent results.

We consider the leading-edge region of a glide vehicle of fixed geometry using variable internal coolant flow over a variable chordwise distance as necessary to hold the temperature of the wing leading-edge region to the design value permitted by the material used. For a specified speed at the start of the glide, we obtain the following approximate relations for the coolant weight fraction:

Laminar heating of leading edge:

$$\frac{W_c}{W} \propto \frac{L}{D}\left(\frac{r}{(W/S)\ C_L}\right)^{1/2} \tag{1}$$

Laminar heating downstream of "sharp" leading edge:

$$\frac{W_c}{W} \propto \frac{L}{D}\left(\frac{1}{\epsilon T_w{}^4}\right) \tag{2}$$

Turbulent heating downstream of "sharp" leading edge:

$$\frac{W_c}{W} \propto \frac{L}{D}\frac{(W/S)^3}{(\epsilon T_w{}^4)^4} \tag{3}$$

From Eq. (1) we note that least leading-edge coolant-weight fraction is obtained for the "sharpest" possible leading edge and the highest possible wing loading, conditions conveniently compatible with high L/D requirements. For laminar surface heating downstream of a "sharp" leading edge, Eq. (2), the coolant-weight fraction is independent of wing loading and inversely proportional to the heat-radiation rate, $\epsilon T_w{}^4$. (If viscous interaction effects are included, wing loading also appears as a factor.) For the turbulent case the result is strongly dependent on both wing loading and heat radiation rate, according to the third power of W/S and the sixteenth power of T_w.

In Fig. 23 we show typical results for a 75-ft-long vehicle with $L/D = 4$, $r = \frac{1}{4}$ in., $\Lambda = 78°$, in an equilibrium glide starting at $v_{max} = 18{,}000$ ft/sec. The coolant is presumed to be water which is vaporized, producing a nominal heat capacity of 1,000 Btu/lb. The strong dependence of the heat load on wall temperature is evident. Totally impractical values are indicated for wall temperatures below about 1500°F. However, for the higher temperatures which now appear feasible through the use of properly coated refractory metals, molybdenum or columbium (38), the requirements are quite modest. At 3000°F the total requirement for 40 lb/ft² wing loading for instance is less than 2 percent of the all-up weight. If a more effective coolant were assumed, for example, liquid nitrogen or hydrogen, the weight penalty becomes still smaller. And if the hydrogen were later to be used for air-breathing propulsion obviously no weight should be charged to the coolant itself—only the weight of the distribution and pumping systems would have to be considered.

Both laminar and turbulent coolant levels are shown on Fig. 23 but for wall temperatures of 2500°F or higher there is little likelihood of turbulent flow. The local Reynolds number based on the streamwise length of cooled surface for the case illustrated is only about 100,000 for $T_w = 2{,}500$, a value well below transition Reynolds numbers, and it would be less for higher T_w and higher v_{max}. The maximum surface lengths requiring cooling are generally less than 1 ft.

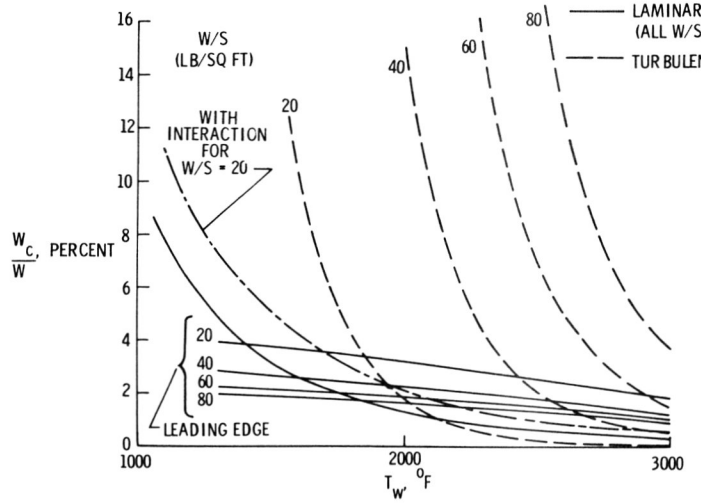

Figure 23. Percent weight increment required to cool leading edge and adjacent undersurface of glide-vehicle wing by internal evaporation of water. $V_{max} = 18{,}000$ ft/sec, $L/D = 4$, $l = 75$ ft, $\Lambda = 78°$.

The mechanical problems of a leading-edge coolant system with its requirement for near-perfect reliability are difficult but certainly no more so than the problems of the cooling system that will be required by air-breathing hypersonic propulsion systems. In fact for airbreathers it is rather obvious that the leading-edge and engine systems can be one and the same. We conclude therefore that sharp-edged high-L/D configurations should not be viewed as structurally impractical; they are in fact attainable through straightforward technological development.

CONCLUSION

Further improvement in hypersonic lift/drag ratios will be difficult to achieve because of the fundamental nature of the obstacles involved. A fruitful area for further research with basic shapes is the little-understood region of low pressure flow on the lee side. Contrary to early assumptions of near-vacuum conditions we find relatively high pressures on the lee side which exert a marked influence on the lift/drag ratio. A knowledge of these real flow details will permit intelligent tailoring of the body shapes to achieve best performance for both the underslung and top-mounted body positions. In the heat-transfer problem special attention should be directed toward improving and validating the semiempirical methods for predicting hypersonic turbulent heating. Transition and heat transfer in transitional hypersonic flows also require high priority research. Finally, a whole new set of problems, together with some interesting new opportunities, arise when an air-ingesting propulsion system is added to the hypersonic configuration problem.

APPENDIX

SYMBOLS

AR	aspect ratio
b	width or span
c	chord length
$\bar{c}$	mean aerodynamic chord
C_L	lift coefficient
$C\mu$	linear viscosity coefficient (Ref. 4)
d	diameter of leading edge
D	drag
l	overall length, or afterbody length
L	lift
$L/D_{\max}$	maximum value of lift/drag ratio
M	flight or free-stream Mach number

N_{St}	Stanton number based on free-stream conditions
p	local pressure
p_∞	free-stream pressure
r	leading-edge radius
R	Reynolds number based on free-stream conditions and overall length l or c
R_x	Reynolds number based on free-stream conditions and length x
$R_{x,l}$	Reynolds number based on local conditions and length x
s	distance along curved surface
s_0	reference distance along curved surface
S	planform area of wing or body
t	maximum thickness
T_w	wall temperature
T_∞	free-stream temperature
v_{max}	maximum velocity of boost-glide vehicle
V	total internal volume
W	gross weight
W_c	total coolant weight
x	streamwise distance
α	angle of attack
α_{opt}	angle of attack for L/D_{max}
α_{sd}	angle of attack for leading-edge shock detachment
ϵ	emissivity coefficient of surface
θ	half-angle of cone
Λ	leading-edge sweepback angle
ϕ	angle between ray from wing apex and wing centerline
$\bar{\chi}$	$\dfrac{M^3\sqrt{C_\mu}}{\sqrt{R_{x=c}}}$

Note: Subscripts FT and FB refer, respectively, to "flat-top" and "flat-bottom" wing-body combinations.

REFERENCES

1. Whitcomb, R., "A Study of the Zero Lift-Drag Rise Characteristics of Wing-Body Combinations Near the Speed of Sound," NACA Report 1273 (1956).
2. Jones, R. T., "Theory of Wing-Body Drag at Supersonic Speeds," NACA Report 1284 (1956).
3. Küchemann, D., "Aircraft Shapes and Their Aerodynamics for Flight at Supersonic Speeds," in *Advances in Aeronautical Sciences*, vol. 3 (New York: Pergamon, 1962).
4. Bertram, Mitchel H., and Arthur Henderson, Jr., "Effects of Boundary-Layer Displacement and Leading-Edge Bluntness on Pressure Distribution Skin Friction, and Heat Transfer of Bodies at Hypersonic Speeds," NACA TN 4301 (1958).

5. Bertram, Mitchel H., and Thomas A. Blackstock, "Some Simple Solutions to the Problem of Predicting Boundary-Layer Self-Induced Pressures," NASA TN D-798 (1961).
6. White, Frank M., Jr., "Hypersonic Laminar Viscous Interactions on Inclined Flat Plates," *ARS J.*, vol. 12, no. 5 (May 1962).
7. Monaghan, R. J., "On the Behavior of Boundary Layers at Supersonic Speeds" (Fifth Int. Aero. Conference, Los Angeles, Calif., June 1955), *Inst. Aero. Sci.* (1955), pp. 277–315.
8. Resnikoff, M. M., "Optimum Lifting Bodies at High Supersonic Air Speeds," NACA RM A54B15 (May 1954).
9. Townsend, L. H., "On Lifting Bodies Which Contain Two-Dimensional Supersonic Flows," Report Aero. 2675, Royal Aircraft Establishment, Ministry of Aviation, London (August 1963).
10. Connors, J. F., and R. C. Meyer, "Design Criteria for Axisymmetric and Two-Dimensional Supersonic Inlets and Exits," NACA TN 3589 (1956).
11. Bertram, M. H., and W. D. McCauley, "An Investigation of the Aerodynamic Characteristics of Thin Delta Wings with Symmetrical Double-Wedge Section at a Mach Number of 6.9," NACA RM L55B14 (April 1955).
12. McLellan, C. H., M. H. Bertram, and J. A. Moore, "An Investigation of Four Wings of Square Plan Form at a Mach Number of 6.9 in the Langley 11-Inch Hypersonic Tunnel," NACA Report No. 1310 (1957).
13. Penland, Jim A., "Aerodynamic Force Characteristics of a Series of Lifting Cone and Cone-Cylinder Configurations at a Mach Number of 6.83 and Angles of Attack up to 130°," NASA TN D-840 (June 1961).
14. Wells, W. R., and W. O. Armstrong, "Tables of Aerodynamic Coefficients Obtained from Developed Newtonian Expressions for Complete and Partial Conic and Spheric Bodies at Combined Angles of Attack and Sideslip with Some Comparisons with Hypersonic Experimental Data," NASA TR R-127 (1962).
15. Miele, A., "Optimum Slender Body of Revolution in Newtonian Flow," Boeing Scientific Res. Lab., Flight Sciences Lab. Tech. Report No. 56 (April 1962).
16. Miele, A., "A Study of the Slender Body of Revolution of Minimum Drag Using the Newton-Busemann Pressure Coefficient Laws," Boeing Scientific Res. Lab., Flight Sciences Lab. Tech. Report No. 62 (August 1962).
17. Ridyard, H. W., "The Aerodynamic Characteristics of Two Series of Lifting Bodies at a Mach Number of 6.86," NACA RM L54C15 (May 1954).
18. Love, E. S., and A. Henderson, Jr., "Some Aspects of Air-Helium Simulation and Hypersonic Approximations," NASA TN D-49 (October 1959).
19. Ladson, C. L., and T. A. Blackstock, "Air-Helium Simulation of the Aerodynamic Force Coefficients of Cones at Hypersonic Speeds," NASA TN D-1473 (October 1962).
20. Blackstock, T. A., and C. L. Ladson, "Comparison of the Hypersonic Aerodynamic Characteristics of Some Simple Winged Shapes in Air and Helium," NASA TN D-2328 (1964).
21. Eggers, A. J., Jr., M. Resnikoff, and D. H. Dennis, "Bodies of Revolution Having Minimum Drag at High Supersonic Speeds," NACA TN 3666 (February 1956).
22. Geiger, R. E., "Experimental Lift and Drag of a Series of Glide Configurations at Mach Numbers of 12.6 and 17.5," *J. Aero. Sci.*, vol. 29, no. 4 (April 1962).
23. Wallace, A. R., and L. G. Siler, "Longitudinal Force Characteristics of Two ASD MDF-4 High Lift-to-Drag Configurations at Mach Number 19," U. S. Air Force, AEDC TDR-64-69 (April 1964).

24. Ferri, A., J. H. Clark, and A. Cassacio, "Drag Reduction in Lifting Systems by Advantageous Use of Interference," PIBAL Report 272, Polytechnic Inst. of Brooklyn (May 1955).
25. Eggers, A. J., Jr., and C. A. Syvertson, "Aircraft Configurations Developing High Lift-to-Drag Ratios at High Supersonic Speeds," NACA RM A55L05, (March 1956).
26. Mead, H. R., F. Koch, and S. A. Hartofilis, "Theoretical Predictions of Pressures in Hypersonic Flow with Special Reference to Configurations Having Attached Leading-Edge Shock," Aeronautical Systems Div., U. S. Air Force, ASD TR 61-60, Parts II and III (October 1962).
27. Bertram, M. H., D. E. Fetterman, and J. R. Henry, "The Aerodynamics of Hypersonic Cruising and Boost Vehicles," NASA SP-23 (December 1962).
28. Goebel, T. P., J. J. Martin, and J. A. Boyd, "Factors Affecting Lift/Drag Ratios at Mach Numbers from 5 to 20," *AIAA J.*, vol. 1, no. 3 (March 1963).
29. Bertram, M. H., and W. D. McCauley, "Investigation of the Aerodynamic Characteristics at High Supersonic Mach Numbers of a Family of Delta Wings Having Double-Wedge Sections with the Maximum Thickness at 0.18 Chord," NACA RM L54G28 (October 1954).
30. Savin, Raymond C., "Approximate Solutions for the Flow About Flat Top Wing-Body Configurations at High Supersonic Air Speeds," NACA RM A58F02 (September 1958).
31. Reshotko, E., "Laminar Boundary Layer with Heat Transfer on a Cone at Angle of Attack in a Supersonic Stream," NACA TN 4152 (1957).
32. Hayes, W. D., and R. F. Probstein, *Hypersonic Flow Theory* (New York: Academic, 1959).
33. Dorodnitsyn, A. A., Proceedings of International Congress on Applied Mechanics, Brussels (1957).
34. Vaglio-Laurin, R., "Supersonic Flow About General Three-Dimensional Blunt Bodies," vol. I: *Inviscid Supersonic Flow About General Three-Dimensional Blunt Bodies*, Aeronautical Systems Div., Wright-Patterson AFB, ASD-TR-61-727, vol. 1 (October 1962).
35. Cooke, J. C., and M. G. Hall, "Boundary Layers in Three Dimensions," AGARD Report 273 (April 1960).
36. Beckwith, I. E., "Similarity Solutions for Small Cross-Flows in Laminar Compressible Boundary Layers," NASA TR R-107 (1961).
37. Stainback, P. C., "An Experimental Investigation at a Mach Number of 4.95 of Flow in the Vicinity of a 90° Interior Corner Alined with the Free-Stream Velocity," NASA TN D-184 (February 1960).
38. Dukes, W. H., and F. M. Anthony, "Thermal Protection of Lifting Reentry Vehicles," *Aerospace Eng.*, vol. 22, no. 1 (January 1963).

ACKNOWLEDGMENT

The author is indebted to the several Langley investigators who have been named at appropriate points in the text for much of the material used in this paper.

COMMENTARY

H. H. PEARCEY (*National Physical Laboratory, Teddington, England*): I was extremely interested in the results for the caret wing that Mr. Becker included with the wealth of his other results. I have not been directly concerned with the work on these configurations in the United Kingdom and it is a pity that the people who have been so concerned are not here, because I feel sure that they would have some interesting comments to make. In their absence, here are some that occur to me. Would Mr. Becker agree that he tried the simplest possible form of this concept of using the pressure field of an entirely attached oblique shock, and that this form is not necessarily the optimum application of the concept to give high L/D for a given value of the volume parameter? Also, the advocates of this principle have perhaps been more concerned with optimising the whole vehicle and not just its L/D. For example, if one considers the desirability of flying it as an aircraft with conventional takeoff and landing, it is possible to design these "caret" or "wave-rider" configurations to achieve good airfield performance without the variable geometry that would, one suspects, be needed for the low aspect-ratio slabs or for the increasingly slender deltas that are based on sonic-leading-edge concepts. Again, I wonder whether Mr. Becker has analysed his excellent and revealing heat-transfer measurements with a view to optimising between good L/D and low total heat intake, or low coolant weight. Here the wave-riders may show up to advantage because one feature of the principle on which they are based is that a given lift is obtained with a uniform pressure over the whole lower surface. Hence they avoid the relatively high local pressures—and the relatively high local heating-rates that go with them—that occur on other configurations which obtain the same lift with a nonuniform distribution of pressure. It is furthermore significant that these relatively high local heating rates tend, embarrassingly, to occur near the leading edge.

REPLY

I would like to thank Dr. Pearcey for calling attention to the fact that our experimental comparisons considered only the simple conceptual form of the caret wing. We have not yet examined any of the more sophisticated forms, nor have we attempted any "trade-off" studies between L/D and structural heat-protection weights. A quick comparison of the Mach 4 pressure distributions of caret wings shows a real advantage over the pressure diagrams for a comparable flat delta. Of course, at hypersonic speeds viscous effects which are present for all wings will tend to reduce this advantage of the caret wing.

COMMENTARY

DR. C. A. LINDLEY (*Aerospace Corporation, El Segundo, Calif.*): The heat transfer data you have shown for the turbulent boundary layer of very efficient aerodynamic configurations should be of great interest to the structural and design

engineer, and others. However, there appears to be a reasonable chance that the boundary layer may be laminar to a very high Reynolds number in the higher speed regimes discussed, unless transition is induced by shock-boundary layer interaction, or other effects of a complex shape. Since the aerodynamic benefits of complex shapes seem to be so small and so equivocal, might it not be wise to concentrate future effort on simple shapes and those conducive to delayed transition?

(The author replied to the effect that the experimental evidence at Mach 6–10 [see Fig. 15] indicated transition at relatively low Reynolds numbers.)

Later Question: In the subsonic regime, we found that wind-tunnel results predicted transition at lower Reynolds numbers than experienced in free flight, unless extreme attention was given to wind-tunnel design. Should we not expect the same in the supersonic regime?

REPLY

One cannot argue with Dr. Lindley's suggestion to choose the simpler shapes which have a better chance of achieving laminar flows, other factors being equal. We must remember, however, that the Reynolds numbers of the Mach 5–8 cruise vehicles will be very high, 100 million or greater. Of greater importance is the extremely irregular nature of the high-temperature heat-protective exterior surface that will exist on these aircraft if their construction follows the methods which now appear most likely. For these reasons, we regard the attainment of extensive laminar flows highly unlikely even for the most favorable shapes. This situation parallels experience with operational subsonic aircraft of the past 30 years which has shown that the extensive laminar flows known to be achievable with ideally smooth surfaces do not occur in the presence of surface manufacturing irregularities or ordinary dirt accretions.

High-L/D reentry vehicles, primarily by virtue of the much lower Reynolds numbers at which they will operate, may derive substantial advantages from laminar flow. In any event, research attention must be directed to the question of hypersonic transition and the effects of surface irregularities because the leading edges of both classes of vehicle will hopefully enjoy laminar flow, and the critical heating regions immediately downstream of the leading edges will be importantly affected by transitional heating phenomena which at present are largely unknown both in character and extent at hypersonic speeds.